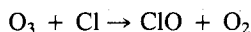


# Reports

## Chlorine Oxide in the Stratospheric Ozone Layer: Ground-Based Detection and Measurement

**Abstract.** *Stratospheric chlorine oxide, a significant intermediate product in the catalytic destruction of ozone by atomic chlorine, has been detected and measured by a ground-based 204-gigahertz, millimeter-wave receiver. Data taken at latitude 42°N on 17 days between 10 January and 18 February 1980 yield an average chlorine oxide column density of  $\sim 1.05 \times 10^{14}$  per square centimeter or  $\sim 2/3$  that of the average of eight in situ balloon flight measurements (excluding the anomalously high data of 14 July 1977) made over the past 4 years at 32°N. We find less chlorine oxide below 35 kilometers and a larger vertical gradient than predicted by theoretical models of the stratospheric ozone layer.*

Measurement of the stratospheric concentration and distribution of ClO is the single best indicator of the depletion of stratospheric O<sub>3</sub> by means of the catalytic cycle (1)



resulting in the conversion of O and O<sub>3</sub> to O<sub>2</sub>. Thus far, balloon-borne in situ measurements made by Anderson and his co-workers (2, 3) over the past several years have provided the only substantial body of positive observational data on which to base assessments to the O<sub>3</sub>

depletion rate by this mechanism. These data, acquired through a series of about a dozen balloon flights reaching maximum altitudes of  $\sim 40$  km typically show a steeper gradient in ClO concentration versus altitude than predicted by existing one- and two-dimensional stratospheric models. A puzzling feature of these data has been the appearance of large ( $\geq$  a factor of 5) variations in ClO concentration with little or no obvious seasonal pattern. An alternative measurement technique, which gives data on the vertical profile, allows economical sampling on a more frequent basis, includes cover-

age of the upper stratosphere, and can be used at sites at various latitudes would thus seem to be desirable.

We report here the first ground-based, remote-sensing measurement of stratospheric ClO, made by adapting techniques and equipment developed for millimeter-wavelength radio astronomy to observe the  $J = 11/2 \rightarrow 9/2$  rotational transition of <sup>35</sup>ClO in emission at 204.352 GHz. The apparatus consists of a millimeter-wave superheterodyne receiver (4) used in conjunction with a filterbank spectrometer of 256 channels, each having a 1-MHz width. The receiving antenna is a small horn fitted with a Teflon lens, which limits the sky view to a symmetric cone with a full angular width of 6.3° measured at the 0.5-power response level and  $< 15^\circ$  at the 0.01-power level.

In our observing procedure we use a beam-deflecting mirror (in the form of a rotating chopper wheel), which causes rapid, repetitive switching of the antenna beam between *S* (for signal; low elevation and hence long stratospheric path length) and *R* (for reference; high elevation and hence short path length) inputs to the detector (5). The quantity  $(S - R)/R$  is computed for each channel on every cycle of the chopper and accumulated as data stored in 10-minute blocks.

Following the common practice in millimeter-wave radio astronomy, we express signal strength as a temperature in kelvins (6). The relation between radiated intensity per unit bandwidth  $I_\nu$  and temperature  $T$  is given in the Rayleigh-Jeans limit by  $I_\nu = 2kT/\lambda^2$ , where  $\lambda$  is the wavelength and  $k$  is Boltzmann's constant.

We have chosen to present our intensity results in the form of the antenna temperature  $T_z^*$ , which is the Rayleigh-Jeans temperature corresponding to the intensity that would be observed if the antenna were pointing toward the zenith, with no attenuation of the line by the troposphere. The conversion from the observed dimensionless  $(S - R)/R$  to  $T_z^*$  in temperature units follows from an analysis of the observing procedure, the geometry of the experiment, and frequent measurements of instrumental noise temperature and atmospheric opacity. Details are given in (7).

The spectral line shape for rotational transitions in ClO is almost completely dominated by collisional pressure-broadening below an altitude of 70 km. Since pressure-broadening is a known function of altitude, an observed peak intensity and line shape contains information about the total quantity and vertical dis-

Table 1. Comparison between observed and predicted spectral line of stratospheric ClO at 204 GHz.

Source	Figure	$\Delta T$ (peak)* (millikelvins)	Line width* (MHz)	ClO column density ( $10^{14}$ cm <sup>-2</sup> )	
				30 to 50 km	24 to 50 km
This study	1a	$21 \pm 2.5$	$31 \pm 5$	0.9†	1.05†
Theoretical models					
Logan <i>et al.</i> (11), "wet" model	1b	35	44	1.77	2.85
Sze and Ko (12)	1c	24	46	1.25	1.86
Crutzen (14)	1d	11	40	0.52	0.78
In situ measurement					
Anderson <i>et al.</i> (2, 13)					
Eight-flight average‡	1e	27	38	1.27	1.62
Seven-flight average‡		26	32	1.10	1.30
Highest, 14 July 1977§	1g	170	42	7.1	9.0
Remote infrared§					
Menzies (16)	1g	70	41	2.4	2.5

\*The value listed for the models is the difference between the predicted intensity at the line center and at  $\pm 80$  MHz away from the center. The true peak intensity for the models is  $\Delta T$  (peak) plus the line wing zero offset shown in Fig. 1, b through e. The line width is the full width measured where the intensity is  $\Delta T$  (peak)/2 above that at  $\pm 80$  MHz from the line center. The values of  $\Delta T$  (peak) and the line width for our data, and their errors, have been determined by a least-squares fitting to the unsmoothed data. Systematic calibration errors will affect the observed peak intensity but not the line width. †The column densities quoted for our data are derived from a distribution of ClO versus altitude whose shape (that of the seven-balloon flight average) with extrapolation beyond 42 km gives good agreement with the observed line width and whose amplitude has been adjusted to give the best least-squares fit to the data over the entire spectral line (Fig. 1f). Curve f in Fig. 2 shows the resulting ClO altitude distribution. ‡The intensities and column densities quoted for these observed ClO distributions include the effect of an extrapolation to higher altitudes than those for which actual measurements were made. The extrapolation used is shown in Fig. 2. §Amplitudes are derived from vertical profiles truncated at  $\sim 40$  km (limit of observed data) and are therefore underestimated.

tribution profile of ClO. Although it is well known that inversion of even a high-quality spectral line shape generally does not yield an unambiguous choice for the shape of the vertical distribution (8), a given vertical profile does unambiguously yield a specific spectral line shape. Hence a comparison between calculated line shapes and observed data can provide a basis for judging the validity of one modeled vertical profile against another.

We present in Fig. 1a data averaged over 17 days of observation from 10 January to 18 February 1980, taken at the Five College Radio Astronomy Observatory near Amherst, Massachusetts (42.4°N latitude). On most days, data were collected between roughly 10 a.m. and 4 p.m., local time. For comparison with theoretical stratospheric models and earlier measurements, computed line shapes are matched against our data in Fig. 1, b through g. These line shapes are generated from the corresponding vertical mixing ratio profiles shown in Fig. 2. In these computations, we have used the temperature and pressure profiles from the 1976 U.S. Standard Atmosphere (9) and the recently measured (10) collisional parameter and temperature dependence of 3.5 MHz/mbar and  $T^{-0.75}$  for the 204-GHz ClO line. Hyperfine splitting has been included in the line shapes, and the amplitude takes into account the 75 percent isotopic abundance of  $^{35}\text{ClO}$ .

In order to compare the data with predictions from the models, we have in each case fitted the experimental line shape by a linear least-squares procedure to the corresponding computed shape over the line wings ( $> 50$  MHz from the line center). This determines an offset, typically several millidegrees off the nominal zero level of our data (see Fig. 1). For a fair comparison of observed and predicted spectral lines, we have thus defined peak intensity and line width relative to the least-squares base line through the line wing at  $\pm 80$  MHz from the line center. In Table 1 we summarize this predicted intensity  $\Delta T$  and line width for the data and the models. A summary of the total column density of ClO for the models is also given in Table 1; this quantity is derived from the vertical profiles of Fig. 2.

Three theoretical models are considered for comparison: (i) the "wet" model of Logan *et al.* (11) (Fig. 1b); (ii) a recent model by Sze and Ko (12) (Fig. 1c), which incorporates a later compilation (13) of reaction rate coefficients (the predicted ClO profile is similar to the "dry" model of Logan *et al.*); and (iii) a

recent model by Crutzen (14) (Fig. 1d). The wet model is inconsistent with the data; it predicts much greater emission than observed at all frequencies across the spectral line, lying about 4 standard deviations above the data. The model-predicted line width (see Table 1) is also much larger than that from the data. The model of Sze and Ko yields a closer fit to the data (Fig. 1c) with good agreement in peak intensity  $\Delta T$  but the observed spectral line still appears significantly narrower, an indication that there is less ClO than would be predicted by the model in the altitude range  $\sim 30 \leq h \leq 36$  km, which contributes strongly to emission 20 to 50 MHz from the line center.

The above models are one-dimensional and apply more appropriately to summer conditions at latitude  $\sim 32^\circ\text{N}$  than to winter at  $42^\circ\text{N}$ . The predictions of the Crutzen model (Figs. 1d and 2) follow from a two-dimensional transport treatment adjusted to February at  $\sim 42^\circ\text{N}$ . The predicted total column density of ClO is about 25 percent of the model of Logan *et al.* and 40 percent of the model of Sze and Ko, in large part arising from the assumption of less total chlorine above 20 km than present in the two one-dimensional models. The spectral line

corresponding to Crutzen's model has a peak intensity  $\sim 1/2$  and a line width  $\sim 4/3$  of those observed. All three theoretical models thus predict a spectral line with a greater width than observed, indicating that the observed altitude distribution has a steeper gradient below  $\sim 36$  km than is found in the theoretical altitude profiles (see Fig. 2).

A comparison between the average ClO line shape deduced from balloon-flight measurements by Anderson *et al.* (2, 3) and the millimeter-wave average is shown in Fig. 1e. In computing line shapes from the balloon measurements, it is necessary to extrapolate above 40 km to allow comparison with our data, which contains a contribution from ClO above 40 km. We have found that extrapolating the mixing ratio (see Fig. 2) smoothly from the data along the upper range of prevailing theories (13) leads to a predicted spectral line with a narrower line width and in better agreement with our data than extrapolating to low ClO mixing ratios. An average from eight balloon flights (13), excluding the anomalously high measurement of 14 July 1977, yields a computed spectral line that is stronger and broader than our measured average (Fig. 1e and Table 1). A substantial improvement is obtained

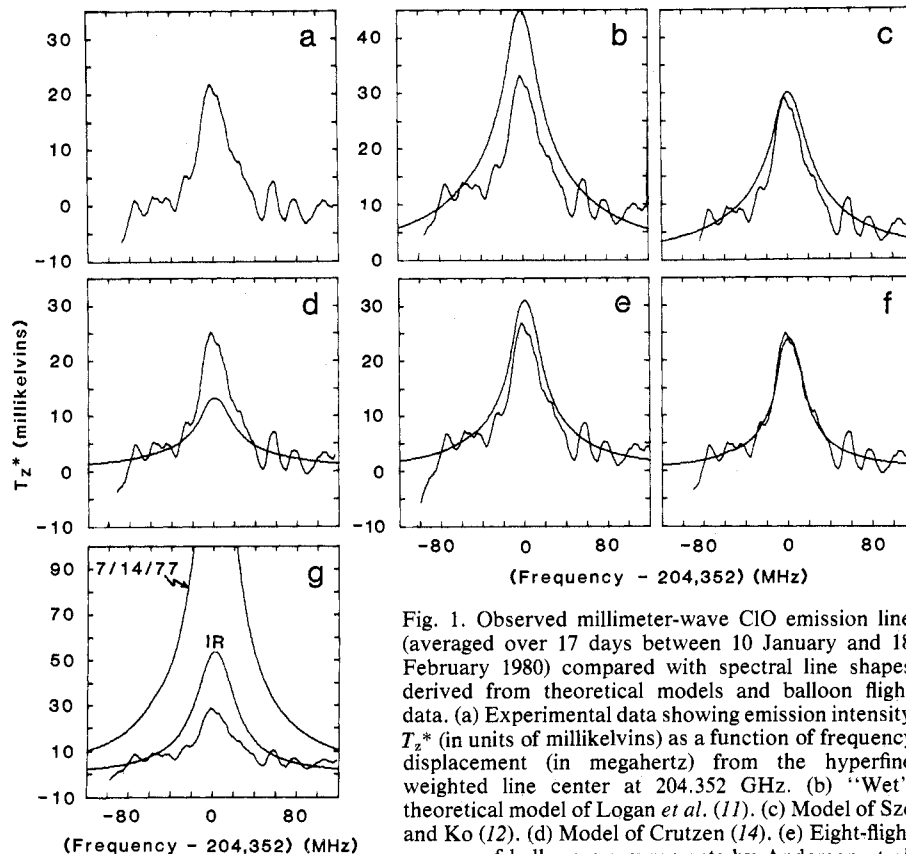


Fig. 1. Observed millimeter-wave ClO emission line (averaged over 17 days between 10 January and 18 February 1980) compared with spectral line shapes derived from theoretical models and balloon flight data. (a) Experimental data showing emission intensity  $T_z^*$  (in units of millikelvins) as a function of frequency displacement (in megahertz) from the hyperfine weighted line center at 204.352 GHz. (b) "Wet" theoretical model of Logan *et al.* (11). (c) Model of Sze and Ko (12). (d) Model of Crutzen (14). (e) Eight-flight average of balloon measurements by Anderson *et al.* (13). (f) Seven-flight average of balloon data scaled by 0.80 (see text). (g) In situ balloon data of 14 July 1977 (2) and remote infrared (IR) data of Menzies (16). Data have been fitted to curves b through e over the same interval in the line wings.

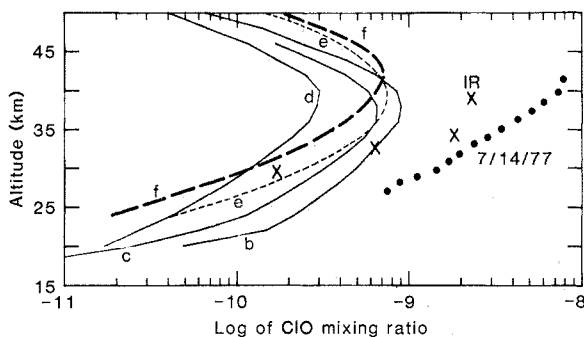


Fig. 2. Altitude distributions used to generate line shapes b through g shown in Fig. 1.

by dropping also the atypically high results of the 28 July 1976 balloon flight. The resulting seven-flight average yields a line width nearly identical to the measured line (Table 1). In Fig. 1f we show a least-squares fit over the entire spectral line of our data and the line shape calculated from the seven-flight average. The fitting requires that the amplitude of the line shape be scaled by a factor of 0.8, but this is well within the combined calibration uncertainties in both sets of data. The zero level offset is found to be 3 millikelvins (Fig. 1f).

The resulting zenith column density (number of CIO molecules included in a vertical column 1 cm<sup>2</sup> in cross section) from the best-fit vertical profile is  $N_z(\text{CIO}) = 0.9 \times 10^{14}$  cm<sup>-2</sup> integrated from 30 km upward, and  $1.05 \times 10^{14}$  cm<sup>-2</sup> from 24 km upward. This determination of column density is not very sensitive to moderate changes in the shape of the altitude distribution; a best fit to the shape derived from the eight-flight average yields a scale factor of 0.70 and column densities of  $0.89 \times 10^{14}$  and  $1.13 \times 10^{14}$  cm<sup>-2</sup> above 30 and 24 km, respectively. Moreover, in either case, extrapolation to high altitude even along the lower range of theories affects the determination of the column density, if we use the best-fit procedure, by less than 5 percent. If model amplitudes are fitted by least-squares procedures to our data across the full line to determine appropriate rescaling of the modeled volume mixing ratios, then all rescaled vertical profiles cross at a mixing ratio  $\approx 0.5$  parts per billion (ppb) at  $\sim 38$  km.

We estimate that the possible systematic calibration error in our data is less than 25 percent. Our finding of substantially less than 1-ppb volume mixing ratio of CIO in the 35- to 40-km range is consistent with the 1-ppb upper limit found by Waters *et al.* (15) in their airborne search for millimeter-wave emission from stratospheric CIO.

At no time during our observing period (including some days during March and April when poorer quality data were

taken) did we find evidence for CIO concentrations approaching the high value found (2) on 14 July 1977 or those of the infrared experiment of Menzies (16). The spectral lines expected from these CIO concentrations are shown in Fig. 1g. A concentration as high as that reported for 14 July 1977 would have been detectable by our system in any 20-minute block of data. No single day of our observations exceeded the average by more than a factor of 2.5. Our typical 1-day signal-to-noise ratio is insufficient to permit clear conclusions to be drawn, but we do see tentative evidence for variations on the order of a factor of 2 in total CIO column density around the mean of our observations, occurring at a time scale of a few days. More observations with increased sensitivity (which should be available shortly) are needed to verify this point. Comparable or larger variations have been a typical feature of

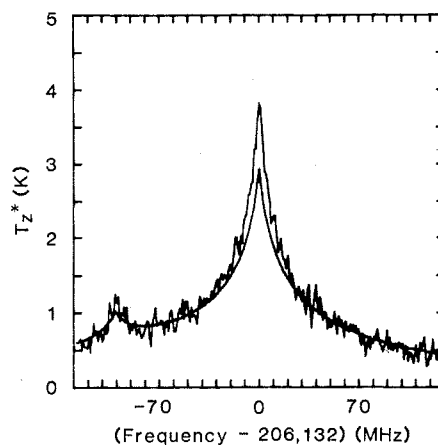


Fig. 3. Intensity scale calibration against O<sub>3</sub> emission lines at 203.452 and 206.132 GHz observed simultaneously in upper and lower side bands. The ordinate is the intensity  $T_z^*$ , and the abscissa is the frequency displacement from the center of the stronger line at 206.132 GHz. The smooth curve is the predicted line shape and intensity computed from the vertical O<sub>3</sub> concentration profile of the 1976 U.S. Standard Atmosphere (seasonal average at  $\sim 45^\circ\text{N}$ ) (9). The same  $T_z^*$  scaling procedure used for CIO data was used to determine the intensity scale for these data. Observing time was 30 minutes.

balloon flight data taken at a much less frequent sampling rate, quite aside from the "anomalously" high value of 14 July 1977.

In summary, we find the CIO distribution in the stratosphere measured at 42°N in the winter to be significantly different from that expected on the basis of several existing theoretical models (all but one of which are intended for summer at  $\sim 32^\circ\text{N}$ ). There is much less CIO at altitudes below 36 km than is predicted in these models. It is not yet clear whether these discrepancies can be accounted for within the framework of two-dimensional models as latitude and seasonal effects or, as seems more likely, by important reaction paths not accounted for in the models. The average column density of CIO that we find for 42°N in January–February is about 20 to 30 percent less than that of the average existing balloon flight measurements (excluding the highest, 14 July 1977) for 32°N, although this disagreement is within the error margin of both experiments.

A. PARRISH

Department of Earth and Space  
Sciences, State University of  
New York, Stony Brook 11794

R. L. DE ZAFRA

Department of Physics, State  
University of New York, Stony Brook

P. M. SOLOMON

J. W. BARRETT

Department of Earth and Space  
Sciences, State University of  
New York, Stony Brook

E. R. CARLSON

Bell Laboratories,  
Holmdel, New Jersey 07733

#### References and Notes

1. F. S. Rowland and M. J. Molina, *Rev. Geophys. Space Phys.* **13**, 1 (1975).
2. J. G. Anderson, H. J. Grassel, R. E. Shetter, J. Margitan, *J. Geophys. Res.* **85**, 2869 (1980).
3. J. G. Anderson, J. J. Margitan, D. H. Stedman, *Science* **198**, 501 (1977).
4. E. R. Carlson, M. V. Schneider, T. F. McMaster, *IEEE Trans. Microwave Theory Tech.* **26**, 706 (1978).
5. The equalization of broadband emission in the S and R beams is necessary to eliminate instrumental effects due to slight nonlinearities typical of the receiving electronics. A millimeter-wave partial absorber is thus mounted in the R beam to add a sufficient amount of broadband emission to compensate for the difference in tropospheric emission between the two beams. The absorber is a slightly lossy dielectric, mounted at Brewster's angle to prevent reflections.
6. See, for example, M. L. Meeks, *Methods Exp. Phys.* **12** (Part B), 1 (1976).
7. R. L. de Zafra, A. Parrish, P. M. Solomon, J. W. Barrett, E. R. Carlson, in preparation. An independent calibration is furnished by direct observation of O<sub>3</sub> line intensities at nearby frequencies (Fig. 3).
8. S. Twomey, B. Herman, R. Rabinoff, *J. Atmos. Sci.* **34**, 1085 (1977).
9. *U.S. Standard Atmosphere, 1976* (Publication NOAA-S/T 76-1562, Government Printing Office, Washington, D.C., 1976). We have found that the computed line shape is insensitive to the small differences in total stratospheric gas pressure (P) and temperature (T) that occur between

- winter and summer standard atmospheres. This is due to the very small changes in  $P/T^{0.75}$  which determine the pressure-broadening.
10. D. E. Brinza, H. M. Pickett, E. A. Cohen, paper presented at the Conference on Spectroscopy in Support of Atmospheric Measurements, Sarasota, Fla., 10 to 12 November 1980.
  11. J. A. Logan et al., *Philos. Trans. R. Soc. London* **290**, 187 (1978).
  12. N. Doc Sze and M. K. W. Ko, *Atmos. Environ.*, in press.
  13. *The Stratosphere: Present and Future* (Publication 1049, National Aeronautics and Space Administration, Washington, D.C., 1979), pp. 164–177.
  14. P. Crutzen, personal communication.
  15. J. W. Waters, J. J. Gustinic, R. K. Kakar, H.

- K. Roscoe, P. N. Swanson, T. G. Phillips, T. de Graauw, A. R. Kerr, *J. Geophys. Res.* **84**, 7034 (1979).
16. R. T. Menzies, *Geophys. Res. Lett.* **6**, 151 (1979).
17. We thank W. Klemperer for first directing our attention to the problem of stratospheric ClO measurement. We thank R. Huguenin and the staff of the Five College Radio Astronomy Observatory for their hospitality and assistance. S. Wofsy and N. Doc Sze offered several helpful comments. This research has been supported by the Chemical Manufacturers Association, with additional assistance from NASA through contract JPL 954829.

22 September 1980; revised 9 December 1980

## Brachiopods in Mud: Resolution of a Dilemma

**Abstract.** Assumptions made from studies of sparse living faunas of brachiopods, namely, that they are intolerant of mud, that the free-lying habit is confined to species without pedicles, and that the pedicle of articulate brachiopods is uniform in structure and function, do not withstand critical examination. Studies in New Zealand show that some species in the same area occur in both attached and free-lying populations. Individuals cannot always be differentiated morphologically, but the structure of populations from hard and soft substrates is distinctive. Attachment to a substrate appears to be a larval rather than an adult requirement in most species.

When Thayer (1) asked why brachiopods no longer inhabit mud, he raised the dilemma encountered by all students of brachiopods. All living articulate brachiopods are assumed to be confined to hard substrates and to be immobile suspension feeders. Their abundance in the originally soft sediments of Paleozoic deposits is thus inexplicable in terms of their known distribution in Recent seas and of the supposed requirements of suspension feeding animals. Another conundrum is the temporal distribution of attached and free-lying taxa. In the Paleozoic, pediculate and free-lying taxa were almost equally represented (1). In Recent seas only one species, *Neothyris lenticularis*, is assumed, from the morphological characters of dredged samples, to be free-lying on coarse sand and gravel substrates (2).

Apparent differences in the habit and habitat of Paleozoic and living faunas are reconciled by data from populations investigated in southern New Zealand. In these coastal waters the brachiopods, like their Paleozoic counterparts, are the dominant component of subtidal faunas. Nine species (representing three of the five orders of living brachiopods) occur in ranges of habitats in neighboring but different geological areas. All of these areas were accessible to scuba divers, thus allowing direct sampling and comparative studies of behavior, morphology, distribution, and population structures.

Because of the rarity and relative inaccessibility of brachiopods in modern seas, correlations between structure and

life-style have had to be made from dredge hauls. Thus the characters of differential thickening and small foramen and beak of *N. lenticularis* have been equated with a free-lying existence (3), and the absence of thickening and the possession of a large foramen have been associated with a life of permanent attachment to a hard substrate. These assumptions have also been used to interpret fossil collections (4).

In coastal waters of southern New Zealand, species with characters previously associated with either attachment or free life are found to have both attached and free-lying populations, some of the latter in mud. Two areas have been studied in detail. (i) Long Sound in Preservation Inlet is a fjord with near-vertical granite walls and has a maximum depth of 380 m. The bottom sediments are anaerobic muds and cur-

rents are negligible in the areas sampled. The only available attachment surfaces are the rock walls. (ii) Paterson Inlet is a drowned river valley with a surface area of 65 km<sup>2</sup>. It does not exceed depths of 45 m and provides a variety of habitats. The northern shoreline is largely granite boulders and outcrops, and numerous islands scattered throughout the inlet have rock surfaces. Sediments of shell gravel and sand surround the islands, particularly at the inlet entrance, but most of the floor is mud.

Four species of brachiopods are common to these two areas: *N. lenticularis*, *Terebratella sanguinea*, *T. inconspicua*, and *Notosaria nigricans*. All are attached to subtidal vertical rock walls in Long Sound (Fig. 1). In Paterson Inlet, individuals of *N. nigricans* are found only attached, adult *Neothyris lenticularis* are found only as free-lying individuals, and the two species of *Terebratella* are either attached or free-lying. *Terebratella inconspicua* is predominantly attached to intertidal and subtidal rock outcrops whereas *T. sanguinea* is mainly free-lying. The relative densities of free-lying forms show that the most favored substrate is shell gravel in which each species occurs at average densities of 200 m<sup>-2</sup>. On substrates of coarse sand *N. lenticularis* is the dominant species, whereas *T. sanguinea* dominates on muddy bottoms at an average density of 100 m<sup>-2</sup> (Fig. 2); *T. inconspicua* and *N. lenticularis* each occur at densities of approximately 20 m<sup>-2</sup> (5).

The distributions observed are thus not in accord with the belief that immobile suspension feeders are intolerant of muddy sediments or that free-lying and attached species are morphologically distinct. The question of the origin of the populations is also raised—whether free-lying populations are derived from those on nearby rock walls or recruited to dif-

Fig. 1. In Long Sound, Preservation Inlet, a vertical rock wall (area ~ 1.0 m<sup>2</sup>) at a depth of 20 m supports the brachiopods *Liothyrella neozelanica*, *Terebratella sanguinea*, and *Notosaria nigricans* and the stylasterine coral *Errina novaezelandiae*. [Photo by P. J. Hill]

